New Layered Mixed Metal Phosphonates for High Dielectric−Polymer Composite Materials

P. Barber, H. Houghton, S. Balasubramanian, Y. K. Anguchamy, H. J. Ploehn,* and H.-C. zur Loye*

Department of Chemistry and Biochemistry and Department of Chemical Engineering, University of South Carolina, Columbia, South Carolina 29208

Received November 13, 2008. Revised Manuscript Received January 26, 2009

New layered 1:1 mixed Ba^{2+}/Ti^{4+} metal phosphonates, $BaTi(O_3PC_6H_5)_3$ and $SrTi(O_3PC_6H_5)_3$, have been prepared via a hydrothermal route, in which mixed metal oxides, $BaTiO_3$ and $SrTiO_3$, were reacted with phenyl phosphonic acid. The mixed-metal phosphonates were combined with polystyrene (PS) via a solution route and cast as thin films for dielectric permittivity measurements. The composites exhibit an enhancement in the dielectric permittivity as a function of weight loading relative to the parent mixed metal oxide−PS composites.

1. Introduction

Existing dielectric capacitors have low energy densities, both on a volume and on a mass basis. No current capacitor technology has the combination of energy density, power density, and rate capability desired for portable pulse power systems currently under development or envisioned for the future. The maximum volumetric energy density W (J/cm^3) stored by a dielectric capacitor,

$$W = 0.5\varepsilon_0\varepsilon_r E_{bd}{}^2$$

depends on the relative dielectric permittivity (or dielectric constant, ε_r) and the dielectric breakdown field strength (E_{bd}). The most obvious way to increase W would be to choose dielectric materials with the highest possible breakdown field strength. Many polymers not only have high values of E_{bd} but also provide the additional advantage of processability. Unfortunately, the dielectric constants for polymers are relatively low. Blending high-ε_r inorganic ceramic materials into polymers can lead to higher effective dielectric constants (ε_{eff}) and thus increase the energy density.[1,2]

Many groups have attempted to disperse commercially available, high ε_r ceramic oxides, such as barium titanate, into polymers followed by fabrication of thin films.[3−9] A major problem that develops from high inorganic loadings in polymers is poor dispersion in the polymer matrix. This may result in ε_{eff} values lower than one might expect on the basis of various theoretical models of composite dielectrics. A more serious consequence is the reduction of E_{bd} relative to that of pure polymer resulting from the low breakdown field strength of the defect-rich inorganic filler network. The recent work of Kim et al.[7] has shown that surface modification of $BaTiO_3$ by various organo-phosphonic acids leads to a better dispersion of $BaTiO_3$ particles in the polymer matrix and to a high effective dielectric constant. However, they still report a 50% decrease in breakdown field strength compared to the pure polymer.

Many diverse organic groups can be incorporated into phosphonic acid derivatives, reacted with a transition metal, and crystallized into a layered metal phosphonate structure.[10−12] These layered materials have found a wide variety of applications, ranging from ion exchange materials,[13,14] catalysts,[15,16] dielectric coatings,[17,18] and magnetism.[19−25]

* To whom correspondence should be addressed. Tel: +1-803-777-6916. Fax: +1-803-777-8508. E-mail: zurloye@mail.chem.sc.edu (H.-C.z.L). Tel: +1-803-777-7307. Fax: +1-803-777-8265. E-mail: ploehn@engr.sc.edu (H.J.P.).

(1) Cao, Y.; Irwin, P. C.; Younsi, K. *IEEE Trans. Dielectr. Electr. Insul.* **2004**, *11*, 797.
(2) Nalwa, H. *Handbook of Low and High Dielectric Constant Materials and their Applications*; Academic Press: London, 1999.
(3) Rao, Y.; Wong, C. P. *J. Appl. Polym. Sci.* **2004**, *92*, 2228–2231.
(4) Sivarajan, R.; Shutzberg, B. A.; Huang, C.; Gao, J.; Giannelis, E. P. *IEEE Trans. Adv. Packag.* **2003**, *26*, 17–24.
(5) Ogitani, S.; Bidstrup-Allen, A.; Kohl, P. A. *IEEE Trans. Adv. Packag.* **2000**, *23*, 313–322.
(6) Bai, Y.; Cheng, V.; Bharti, V.; Xu, S.; Zhang, Q. M. *Appl. Phys. Lett.* **2000**, *76*, 3804–3806.
(7) Bhattacharya, S. K.; Tummala, R. R. *J. Mater. Sci. Mater. Electr.* **2000**, *11*, 253.
(8) Windlass, H.; Raj, P. M.; Balaraman, D.; Bhattacharya, S. K.; Tummula, R. R. *IEEE Trans. Adv. Packag.* **2003**, *26*, 10.
(9) Kim, P. J.; Simon, C.; Hotchkiss, P. J.; Haddock, J. N.; Kippelen, B.; Marder, S. R.; Perry, J. W. *Adv. Mater.* **2007**, *19*, 1001–1005.
(10) Clearfield, A. *Curr. Opin. Solid State Mater. Sci.* **1996**, *1*, 268–278.
(11) Clearfield, A. *Curr. Opin. Solid State Mater. Sci.* **2002**, *6*, 495–506.
(12) Mao, J. G. *Corrd. Chem. Rev.* **2007**, *251*, 1493–1520.
(13) Alberti, G.; Casciola, M.; Constantino, U.; Vivani, R. *Adv. Mater.* **1996**, *8*, 291–303.
(14) Wu, Q.; Weiss, R. A. *J. Polym. Sci., Part B: Polym. Phys.* **2004**, *42*, 3628–3641.
(15) Curini, M.; Rosati, O.; Constantino, U. *Curr. Org. Chem.* **2004**, *8*, 591–606.
(16) Zhang, X.-J.; Ma, T.-Y.; Yuan, Z.-Y. *J. Mater. Chem.* **2008**, *18*, 2003–2010.
(17) Katz, H. E.; Schilling, M. L. *Chem. Mater.* **1993**, *5*, 1162–1166.
(18) Schilling, M. L.; Katz, H. E.; Stein, S. M.; Shane, S. F.; Wilson, W. L.; Ungashe, S. B.; Taylor, G. N.; Putvinski, T. M.; Chidsey, C. E. D.; Buratto, S. *Langmuir* **1993**, *9*, 2156–2160.
(19) Bujoli, B.; Pena, O.; Palvadeau, P.; Le Bideau, J.; Payen, C.; Rouxel, J. *Chem. Mater.* **1993**, *5*, 583–587.
(20) Rabu, P.; Janvier, P.; Bujoli, B. *J. Mater. Chem.* **1999**, *9*, 1323–1326.
(21) Bellitto, C.; Bauer, E. M.; Righini, G. *Inorg. Chim. Acta* **2008**, *361*, 3785–3799.
(22) Yao, H.-C.; Li, Y.-Z.; Gao, S.; Song, Y.; Zheng, L.-M.; Xin, X.-Q *J. Solid State Chem.* **2004**, *177*, 4557–4563.
(23) Cao, D.-K.; Xie, X.-J.; Li, Y.-Z.; Zheng, L.-M. *Dalton Trans.* **2008**, *37*, 5008.

10.1021/cm8030945 CCC: $40.75 © 2009 American Chemical Society
Published on Web 03/03/2009

These applications typically require the phosphonate structure to consist of metal layers bonded to the PO_3^{2-} end of the phosphonic acid, with the organic group protruding into the interlayer cavity. One hopes that both the electronic structure and the organic functionality can be tailored to give the desired bulk property.[26]

Metal phosphonate compounds formed with di- and trivalent metal ions have higher solubilities than their tetravalent metal containing counterparts, permitting the crystal growth of di- and trivalent metal phosphonates by slow precipitation routes.[10] The most common structural motif for metal phosphonate compounds is that of a layered structure. In these solids the phosphonate oxygens bond strongly to the metal ions, forming a tightly bound inorganic layer, with the organic groups located between the inorganic lamellae. These inorganic layers can be built from planes of metal atoms with phosphonates lying above and below the plane. The phosphonates are bonded to two or three different metal atoms, and this arrangement forces the phosphorus−carbon bond to be orientated away from the inorganic sheets. This molecular arrangement creates an organic bilayer between the inorganic lamellae, where the segregation of organic and inorganic groups into separate layers is a simple form of molecular engineering.

In our search through the expansive library of synthesized metal phosphonates, in the literature,[10−12] only two reports describing the synthesis of a layered 1:1 mixed-metal phosphonate was found. In these reports, Menaa and Shannon successfully synthesized mixed divalent-metal layered phosphonates through isomorphic substitution.[27,28] To date, however, no one has reported a mixed-metal phosphonate comprised of both a divalent and tetravalent metal in which isomorphic substitution is not possible.

It is known that the use of a complexing agent, such as oxalic acid, can be used to sequentially dissolve mixed metal oxides. Figueroa et al. explored the solubilities of simple metal oxides under aqueous conditions,[29] where oxalic acid was used as a chelating agent that enabled the formation of mixed metal oxalate species. Using this synthetic approach with phosphonic acids, we were able to convert perovskites, such as barium or strontium titanate, into single-phase mixed metal phosphonates that retain the original ratio of metals in the mixed metal oxide starting material. This type of mixed metal phosphonate is of interest for incorporation into polymer composites because the organic groups may promote chemical compatibility with the polymer host, while the metal centers may improve the electronic properties, in particular the dielectric constants, of the composite. This article reports the synthesis of novel layered mixed-metal phosphonates and the effective dielectric constants of polymer composites containing these new materials.

(24) Rabu, P., Drillon, M. *Magnetic organic-inorganic hybrid materials. Synthesis, structures, and properties*; American Scientific Publishers: Stevenson Ranch, CA, 2003; Vol. 1.
(25) Rabu, P., Drillon, M. *Layered organic-inorganic materials. A way towards controlling magnetism*; Wiley: Weinheim, Germany, 2004.
(26) Thompson, M. E. *Chem. Mater.* **1994**, *6*, 1168–1175.
(27) Menaa, B.; Shannon, I. J. *Chem. Eur. J.* **2002**, *8*, 4884–4893.
(28) Menaa, B.; Shannon, I. J. *J. Mater. Chem.* **2002**, *12*, 350–355.
(29) Figueroa, C. A. S. P. J.; Morando, M. A.; Blesa, J. *J. Colloid Interface Sci.* **2000**, *225*, 403.

2. Experimental Section

2.1. Materials. All chemicals were of reagent grade from commercial sources and used without any further purification. Barium and strontium titanate were purchased from Aldrich Chemical Co. (nanopowder, 99+%). Barium nitrate and potassium bis(oxalato)oxotitanate dihydrate (99.95% purity) and polystyrene (nominally 100 000 g/mol) were purchased from Alfa Aesar. Phenyl phosphonic acid (98% purity) was purchased from Acros.

2.2. Structure Characterization. FT-IR spectra were recorded on a Perkin-Elmer Spectrum 100 using an ATR diamond cell attachment.

Powder X-ray diffraction patterns were collected using a Rigaku DMAX 2200 diffractometer using Cu Kα radiation.

Thermogravimetric analyses were performed using a thermal analysis (TA) SDT-Q600 simultaneous DTA/TGA system in an oxidizing environment. Samples were heated in air to 800 °C using a heating rate of 10 °C/min.

Solid-state ^{31}P NMR spectra were collected on a Varian Inova 500 spectrometer operating at 202.489 MHz using a Doty Scientific 4 mm/XC magic angle spinning (MAS) probe. Bloch decays of 50 ms were collected with a 200 ppm window after 45° excitation pulses. A relaxation delay of 10 s was used between each transient. TPPM dipolar decoupling with a field strength of 45 kHz was applied during acquisition. A MAS speed of 10 kHz was used, and between 16 to 64 scans were collected for each run. Spectral deconvolution was performed with the standard routine included with Varian's VNMR 6.1C software.

Platelet imaging and elemental analyses were collected using a JEOL 2100F 200 kV field-emission gun TEM/STEM with an Oxford Instruments INCA EDS solid-state X-ray detector. XPS measurements were carried out on the Kratos AXIS Ultra DLD XPS system equipped with a hemispherical energy analyzer and a monochromatic Al Kα source. The monochromatic Al Kα source was operated at 15 keV and 180 W. The pass energy was fixed at 40 eV for the detailed scans. Since the sample was nonconductive, a charge neutralizer was used to neutralize the charge during XPS measurement.

Capacitance measurements at 100 kHz and 1 MHz were made using a Keithley 590 CV analyzer instrument.

2.3. Synthesis of $BaTi(C_6H_5PO_3)_3$ and $SrTi(C_6H_5PO_3)_3$ [$BaTi(PPA)_3$ and $SrTi(PPA)_3$]. $BaTi(C_6H_5PO_3)_3$ and $SrTi(C_6H_5PO_3)_3$ were synthesized via a hydrothermal route. One millimole of $BaTiO_3$ or $SrTiO_3$ was added to 25 mL of a 0.125 M solution of phenyl phosphonic acid, $C_6H_5PO_3H_2$, and the reaction mixture was sealed in a Teflon lined steel autoclave. The autoclave was heated to 150 °C for 72 h. The resulting white powders were filtered via vacuum filtration and washed with ethanol to remove unreacted reagents. The samples were dried in a convection oven overnight at 80 °C. For convenience, we will refer to these products as $BaTi(PPA)_3$ and $SrTi(PPA)_3$.

2.4. Synthesis of $Ba(C_6H_5PO_3)\cdot H_2O$ and $Ti(C_6H_5PO_3)_2$ [Ba(PPA) and $Ti(PPA)_2$]. The syntheses of divalent and tetravalent metal phosphonates are well established and are described elsewhere in detail.[30,31] In brief, stoichiometric mixtures of the specific metal salt and PPA were dissolved in distilled water. The solutions were sealed in a Teflon-lined steel autoclave and heated to 150 °C for 48 h. Single crystals of the divalent metal phosphonate are normally produced, while white powders of tetravalent metal phosphonate

(30) Anillo, A. A. V.-G.; Maria, A.; Llavona, R.; Suarez, M.; Rodriguez, J. *Mater. Res. Bull.* **1999**, *34*, 627–640.
(31) Cao, G.; Lynch, V. M.; Swinnea, S.; Mallouk, T. *Inorg. Chem.* **1990**, *29*, 2112.

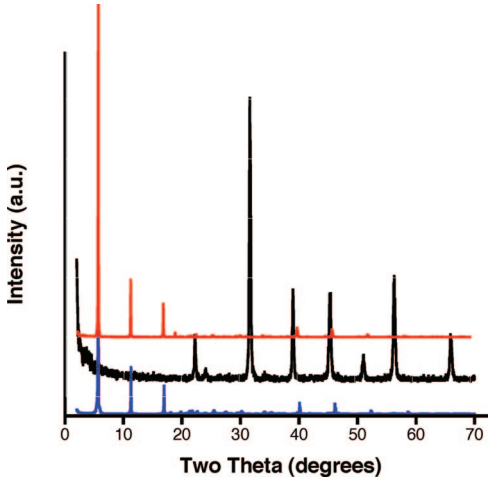

Figure 1. Powder XRD patterns of $BaTiO_3$ (black), $BaTi(PPA)_3$ (blue), and Ba(PPA) (red).

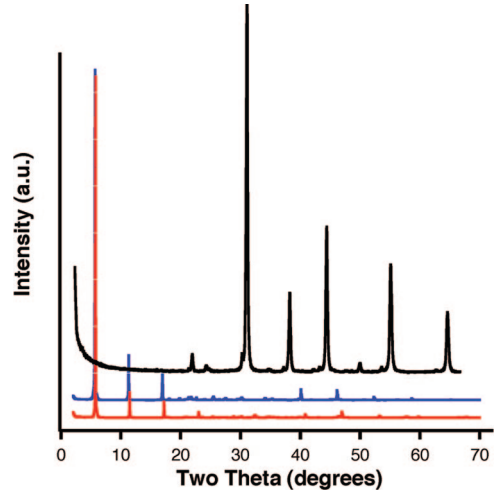

Figure 2. Powder XRD patterns of $BaTi(PPA)_3$ (blue), $SrTi(PPA)_3$ (black), and $SrTiO_3$ (red).

are generated. For convenience, we will refer to these single metal phosphonates as Ba(PPA) and $Ti(PPA)_2$. The characterizations of these known single metal phosphonates are reported in the Supporting Information section.

2.4. Solvothermal Mixture Ba + Ti + PPA. We also attempted to synthesize $BaTi(PPA)_3$ starting with separate barium and titanium sources, $Ba(NO_3)_2$ and $K_2[TiO(C_2O_4)_2]\cdot 2H_2O$, respectively, rather than with a mixed metal precursor, such as $BaTiO_3$. An aqueous solution containing 1 mmol of $Ba(NO_3)_2$, 1 mmol of $K_2[TiO(C_2O_4)_2]\cdot 2H_2O$, and 3.1 mmol of PPA was sealed in a Teflon lined steel autoclave. The autoclave was heated to 150 °C for 72 h. The resulting white powder was washed with ethanol to remove unreacted reagents and dried in a convection oven overnight at 80 °C.

2.5. Preparation of Polystyrene Composite Capacitors. Polystyrene was dissolved in 20 mL of toluene under rigorous magnetic stirring for 4 h. Amounts of inorganic materials ($BaTiO_3$, $SrTiO_3$, $BaTi(PPA)_3$, and $SrTi(PPA)_3$) were added so as to achieve the target weight loading, followed by stirring for 15 h to obtain a slurry. The viscosity of the slurry was adjusted as needed by adding toluene. Thin aluminum foil (average thickness 15 μm) was carefully wrapped around a suitable substrate (silicon or pyrex discs), cleaned with ethanol, and then dried with compressed air. Next, the PS−inorganic slurry was spin-coated on the Al foil with rotation at 1000 rpm for 15 s. The toluene was evaporated from the spin-coated substrate in a vacuum oven at 80 °C for 12 h. Finally, parallel plate capacitors were formed by sputter depositing aluminum or gold as top electrodes onto the film surface through a shadow mask. The underlying Al foil served as the bottom electrode. In general we observe no significant variation in the capacitance between Al−Al and Au−Al capacitors prepared in this way.

3. Results

3.1. Powder X-ray Diffraction. Phase purity of the final products, $BaTi(PPA)_3$ and $SrTi(PPA)_3$, were checked by powder X-ray diffraction. Figures 1 and 2 show the diffraction patterns of the starting materials and the products. The diffraction patterns of $BaTi(PPA)_3$ and $SrTi(PPA)_3$ consist of several evenly spaced low-angle peaks that are characteristic of 00*l* reflections of layered solids. The diffraction lines for $BaTi(PPA)_3$ and $SrTi(PPA)_3$ overlay almost perfectly, indicating that both the compounds are structurally similar. This similarity is to be expected given that both compounds contain the same pendant phenyl group. Furthermore, the slight shift of the $BaTi(PPA)_3$ pattern toward lower angles is consistent with the larger size of barium relative to strontium. Attempts to index the powder X-ray diffraction patterns resulted in an interlayer separation of 15.754(1) Å and 15.351(1) for $BaTi(PPA)_3$ and $SrTi(PPA)_3$, respectively. As a result of preferred orientation, only the first three diffraction lines could be used to index the patterns. The diffraction pattern for the single metal phosphonate, $Ti(PPA)_2$ (see Supporting Information), is featureless, indicating an amorphous structure.[30] Data from NMR, TGA, and XRD of thermal degradation products (vide infra) support the assertion that the reaction product is a mixed metal phosphonate, $BaTi(PPA)_3$, rather than a mixture of layered Ba(PPA) and amorphous $Ti(PPA)_2$.

3.2. Platelet Elemental Analysis with XPS and HRTEM/EDS. To analyze the chemical composition of the mixed-metal phosphonates and to confirm the layered structure of these materials high-resolution transmission electron microscopy (HRTEM) images were collected and energy dispersive spectroscopy (EDS) data for the samples were obtained. EDS was used to determine the metal composition of the mixed metal phosphonates. As a result of the peak overlap associated with Ba and Ti in EDS, which prevents a quantitative analysis, only $SrTi(PPA)_3$ was studied in detail by HRTEM/EDS.

To establish the presence of both strontium and titanium in the same platelet, HRTEM coupled with EDS was carried out on the $SrTi(PPA)_3$ sample dispersed in toluene. Figure 3 shows an HRTEM image of a single platelet of $SrTi(PPA)_3$. The metal composition of the indicated area on the platelet is 51% Sr and 49% Ti. The EDS data collected on several such platelets, summarized in Table 1 (images given in Supporting Information), demonstrate that within experimental error, the ratio of Sr:Ti present in each platelet is 1:1. This is consistent with the result of XPS analysis of the bulk powder (Table 1). Overlap of Ba and Ti peaks in EDS prevents quantitative analysis by the this method; however, XPS analysis of $BaTi(PPA)_3$ does show a 1:1 ratio of metals.

3.3. ^{31}P MAS NMR Experiments. ^{31}P MAS NMR experiments were carried out to investigate the phosphorus

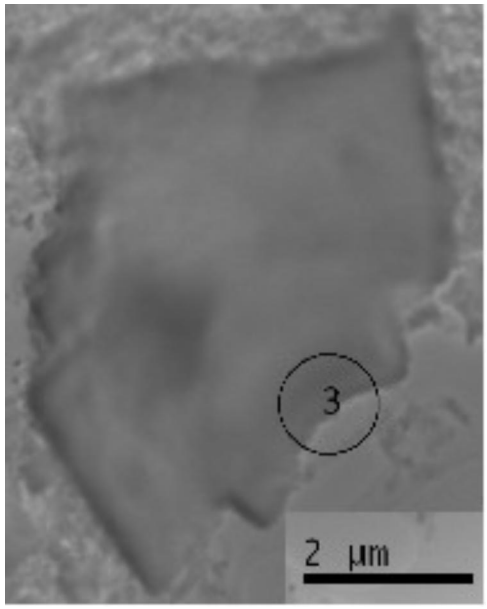

Figure 3. HRTEM imaging of $SrTi(PPA)_3$. The area circled and labeled 3 represents the EDS spectra taken. Other EDS/HRTEM images can be seen in the Supporting Information section.

Table 1. EDS Results for $SrTi(PPA)_3$ Platelets Imaged by HRTEM (Figure 3 and Supplemental Information) and XPS Results for $BaTi(PPA)_3$ and $SrTi(PPA)_3$ Bulk Powders

EDS	atomic % Sr	atomic % Ti
position 1	48.80	51.20
position 3	50.74	49.26
position 4	50.49	49.51
position 5	48.81	51.19
position 6	49.22	50.78
average atomic ratio	49.61± 1	50.38 ± 1

XPS	atomic % Sr (Ba)	atomic % Ti
SrTi(PPA)	48.56±2	51.44±2
BaTi(PPA)	47.64±2	52.36±2

environments in $BaTi(PPA)_3$, in the physical 1:1 mixture of Ba(PPA) and $Ti(PPA)_2$, and in the solvothermal Ba + Ti + PPA product. ^{31}P MAS NMR spectra for the pure metal phosphonates, $Ti(PPA)_2$ and Ba(PPA), were also collected to compare them with the phosphorus environments in the mixed metal samples. The presence of peaks in the ^{31}P MAS NMR spectra provides a qualitative indication of different phosphorus environments in the various samples.

The crystal structures of $Ti(PPA)_2$ [30,32] and Ba(PPA)[34] are shown in Figure 4. The phosphorus environments differ in $Ti(PPA)_2$ vs Ba(PPA). In the $Ti(PPA)_2$ structure, the octahedral coordination sphere around each Ti^{4+} cation consists of six oxygens from six different phosphonate groups; each phosphonate group bridges three Ti^{4+} cations. A consequence of this structural arrangement is that the TiO_6 octahedra are isolated from each other. By comparison, in the Ba(PPA) structure, the coordination environment around each Ba^{2+} cation consists of six oxygens, two of which belong to a single phosphonate group, three of which belong to three other different phosphonate groups, and one that is part of a water molecule; each phosphonate group bridges three Ba^{2+} cations. A consequence of this structural arrangement is that

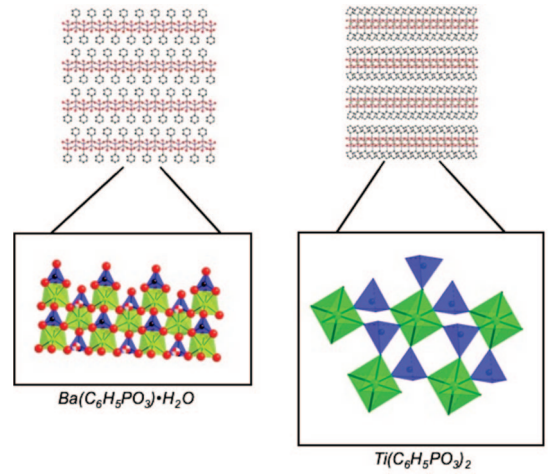

Figure 4. Metal phosphonate framework for Ba(PPA) (left) and $Ti(PPA)_2$ (right). Carbon atoms are shown in black, oxygen atoms in red, metal ions in green, and phosphorus atoms in blue. The oxygen atoms from the coordinated water are shown in striped red-white colors.

each BaO_6 octahedron is connected via a shared oxygen to four other BaO_6 octahedra. In both $Ti(PPA)_2$ and Ba(PPA), the crystal structure suggests that the phosphorus will have a single coordination environment in each of these materials. This is confirmed by the ^{31}P MAS NMR spectra. The ^{31}P resonances in $Ti(PPA)_2$ and Ba(PPA), as shown in Figure 5a,b, occur at −3.92 ppm and 9.25 ppm, respectively, indicating that in each structure there is only a single, unique phosphorus environment.[30] It is important to point out that the chemical shift of 12.40 ppm,[33] observed in the protonated $Ba(C_6H_5PO_3H)_2$, is not seen, and that only the chemical shift of 9.25 ppm, associated with the deprotonated $BaC_6H_5PO_3$, is seen.

In contrast, the ^{31}P MAS NMR experiments indicate that, in $BaTi(PPA)_3$ (Figure 5c), three distinct phosphorus environments are present. The first phosphorus peak at −3.95 ppm (s) corresponds to the $M^{4+}-O-P$ environment found in $Ti(PPA)_2$ as seen in the standard ^{31}P MAS NMR spectrum of pure $Ti(PPA)_2$. Another phosphorus resonance is observed at 9.25 ppm and corresponds to the $M^{2+}-O-P$ environment in Ba−O−P as seen in the standard ^{31}P MAS NMR spectrum of pure Ba(PPA). An integration of the area under the peaks indicates that the resonances correspond to 1/3 Ba−O−P to 2/3 Ti−O−P. This is in good agreement with the expected composition and structure of $BaTi(PPA)_3$, where charge balance would dictate that one PPA group is associated with each divalent barium and two PPA groups are associated with each tetravalent titanium. A third phosphorus resonance is observed at 3.38 ppm in the $BaTi(PPA)_3$ material. This is a new resonance and has no counterpart in either of the single metal phosphonates. The third phosphorus environment, located between the other two phosphorus resonances, is unique to the $BaTi(PPA)_3$ structure and suggests a phosphorus environment influenced by both the titanium and the barium. We believe that this environment corresponds to the phosphonate bridging motif Ba−O−P−O−Ti.

(32) Alberti, G.; Casciola, M. *Inorg. Chim. Acta* **1992**, *201*, 207–212.

(33) Lazarin, A. M.; Airoldi, C. *J. Inclusion Phenom. Macrocyclic Chem.* **2005**, *51*, 33–40.

(34) Svoboda, J.; Zima, V.; Benes, L.; Melanova, K.; Vleck, M.; Trchova, M. *J. Phys. Chem. Solids* **2008**, *69*, 1439.

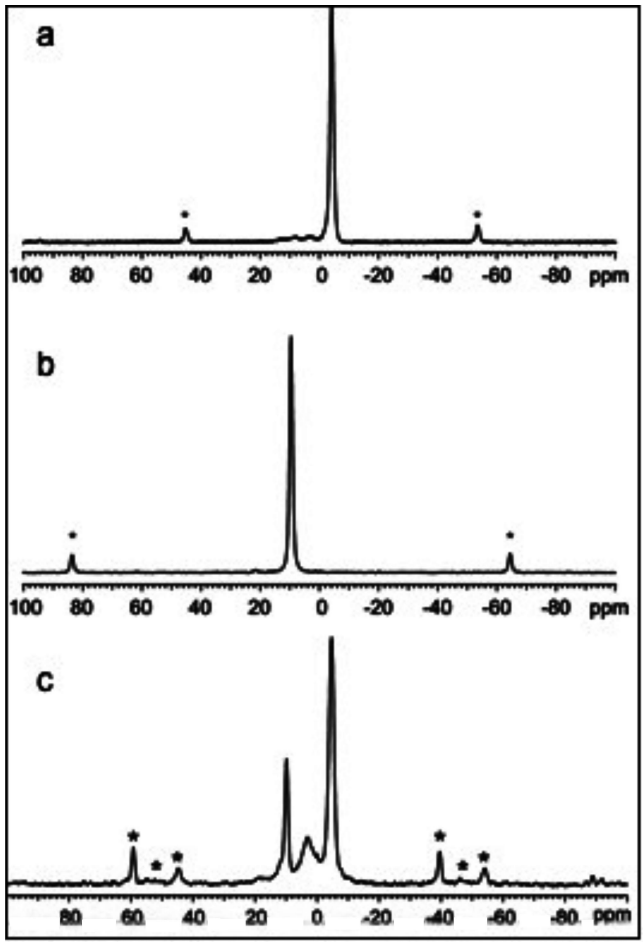

Figure 5. ^{31}P MAS NMR spectra of (a) $Ti(PPA)_2$, (b) Ba(PPA), and (c) $BaTi(PPA)_3$.

Consistent with this assignment of the resonance at 3.38 ppm is the observation that this resonance is not observed in simple physical mixtures of the two individual metal phosphonates. In the ^{31}P spectrum for the physical mixture (Figure 6b), we do not observe the 3.38 ppm resonance, although we do see an additional resonance at 12.40 ppm,[33] as a result of the presence of $Ba(PPAH)_2$, an impurity that forms during the Ba(PPA) synthesis. In the ^{31}P spectrum for the solvothermal mixture, Figure 6c, the 3.38 ppm resonance is again not observed. However, the spectrum does show a strong peak associated with the kinetically favored product, $Ti(PPA)_2$, as well as a weak resonance due to the presence of a small amount of Ba(PPA). (The powder X-ray diffraction pattern of the solvothermal mixture can be found in the Supporting Information).

Analogous results are obtained for $SrTi(PPA)_3$. Figure 7 compares the ^{31}P MAS NMR spectra for $SrTi(PPA)_3$ and $BaTi(PPA)_3$. The ^{31}P MAS NMR spectrum for $SrTi(PPA)_3$ shows three phosphorus environments like $BaTi(PPA)_3$. The first phosphorus environment located at 10.08 ppm relates to the Sr−O−P, and the Ti−O−P environment is located at −4.31 ppm. Similar to the $BaTi(PPA)_3$ material, a third phosphorus environment is seen between the Sr−O−P and the Ti−O−P environments at 3.15 ppm. We believe that this phosphorus environment corresponds to the Sr−O−P−O−Ti bridging motif.

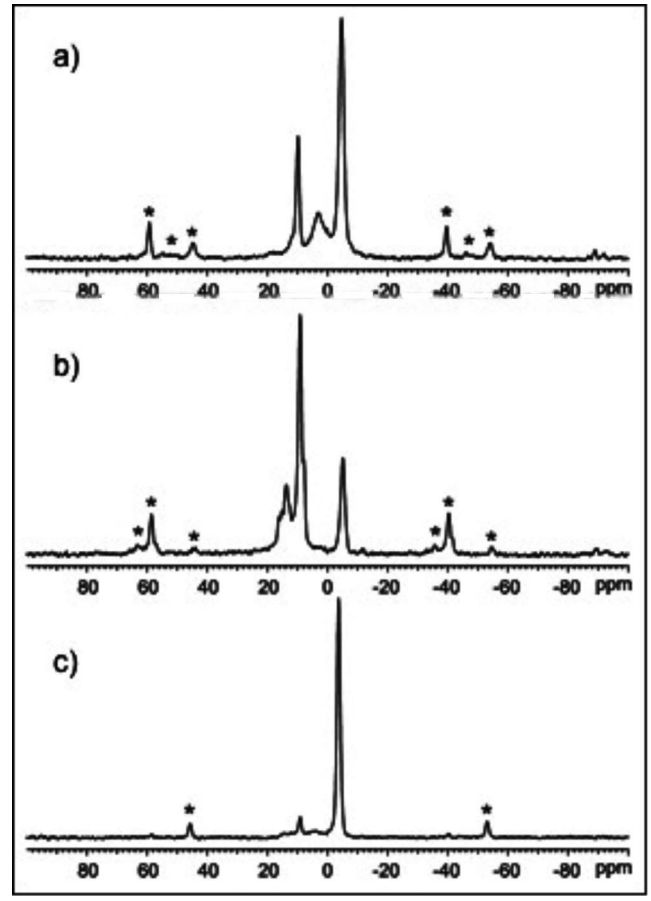

Figure 6. ^{31}P MAS NMR spectra of (a) $BaTi(PPA)_3$, (b) physical mix, and (c) solvothermal mix.

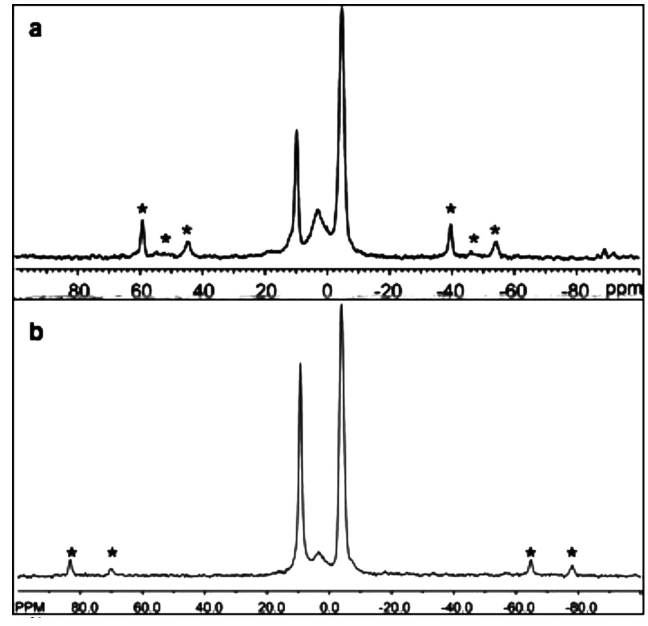

Figure 7. ^{31}P MAS NMR spectra of mixed-metal phosphonates (a) $BaTi(PPA)_3$ and (b) $SrTi(PPA)_3$.

3.4. Thermal Analysis. To study the thermal stability of the mixed metal phosphonates, thermogravimetric analysis experiments were carried out. Thermogravimetric data for thermal degradation of the mixed metal phosphonates (Figure 8) indicate weight losses of 31.1% and 34.3% for $BaTi(PPA)_3$ and $SrTi(PPA)_3$, respectively. On the basis of numerous

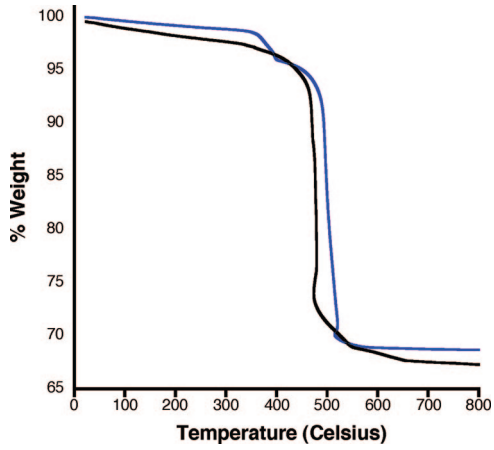

Figure 8. Thermal gravimetric curves of $BaTi(PPA)_3$ (blue) and $SrTi(PPA)_3$ (black).

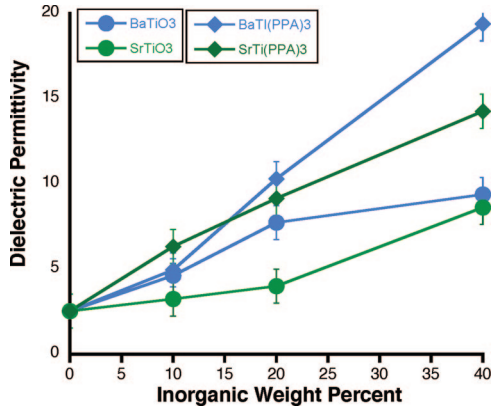

Figure 9. Dielectric constant values of polystyrene composites as a function of weight loading.

literature reports of metal phosphonate thermal degradation,[8,9,20,21] the thermal degradation scheme is expected to be as follows:

$$MTi(C_6H_5PO_3)_3 \xrightarrow[\text{air}]{\text{heat}} MTi(P_2O_7)_{1.5} + 3C_6H_5\uparrow$$

The observed weight loss values are in very good agreement with theoretical weight losses of 31.7% and 34.3% for the formation of $BaTi(P_2O_7)_{1.5}$ and $SrTi(P_2O_7)_{1.5}$, respectively, confirming the metal to phosphonate ratio in these compounds. The greatest amounts of weight losses occurred over a relatively narrow temperature range (500 °C for $SrTi(PPA)_3$ and 525 °C for $BaTi(PPA)_3$).

3.5. Dielectric Properties of Polystyrene Composites. Figure 9 shows the dielectric constant as a function of inorganic weight loading for polystyrene (PS) composites incorporating the two titanates ($BaTiO_3$ and $SrTiO_3$) and the two corresponding mixed metal phosphonates [$BaTi(PPA)_3$ and $SrTi(PPA)_3$]. Each data set also includes the value for pure PS, 2.6 ± 0.1, plotted at 0 wt %. For the titanates, the dielectric constants increase by a factor of nearly four as weight loading increases to 40 wt % (to 9.4 ± 0.5 for $BaTiO_3$ and to 8.6 ± 0.2 for $SrTiO_3$). The dielectric constants of the mixed metal phosphonates also increase considerably with inorganic weight loading and are significantly higher than the corresponding titanates at almost every point. At 40 wt %, the dielectric constant of $SrTi(PPA)_3$ is 66% higher (14.3 ± 0.3) than that of $SrTiO_3$. The dielectric constant of $BaTi(PPA)_3$ is 106% higher (19.4 ± 0.2) than that of $BaTiO_3$ and more than six times greater than the value for pure PS.

It is also interesting to compare the dielectric constant of a single metal phosphonate with that of the mixed metal phosphonate. The dielectric constant of 40 wt % Ba(PPA) in PS, 4.6 ± 0.1, is significantly lower than the values for either $BaTiO_3$/PS or $BaTi(PPA)_3$/PS at the same weight loading. This suggests that significant enhancement of the dielectric constant depends on the presence of the two different metals joined by a "linker" atom in the inorganic phase. Comparing the M−O−Ti motif (M = Ba or Sr) in the titanates with the putative M−O−P−O−Ti motif in the phosphonates, the latter apparently leads to a consistently higher increment in the effective dielectric constant of the PS composite.

4. Discussion

The reaction between the ternary oxides, $BaTiO_3$ and $SrTiO_3$, and phenylphosphonic acid is akin to the well-known dissolution reactions between mixed metal oxides and chelating species, such as oxalic acid, which result in the formation of metal complexes.[29] Moreover, during such dissolution reactions it has been determined that, after an initial incongruent dissolution of a small fraction of the solid, the dissolution becomes congruent and both metals are transferred at the same rate. In the case of the tridentate phosphonic acid species, the resultant product is not a molecular metal complex but rather a mixed-metal extended structure that precipitates out of solution. Furthermore, on the basis of our understanding of the dissolution process, it is not unexpected that the formed metal phosphonate contains both metals in the same ratio as the precursor, $BaTiO_3$, Ba:Ti = 1:1. In fact, a 1:1 metal ratio for the two mixed-metal phosphonates that were prepared from $BaTiO_3$ and $SrTiO_3$ was confirmed by several techniques, including XPS (bulk) and HRTEM/EDS (single platelet). The metal to phosphonic acid ratio, 2:3, was established by both TGA and NMR and is consistent with the charges on the metals (Ba^{2+} and Ti^{4+}) and the charge on the phosphonate (PPA^{2-}). Hence, we believe that the mixed metal phosphonates prepared by this synthetic route have compositions of $BaTi(PPA)_3$ and $SrTi(PPA)_3$.

The structure of these mixed metal phosphates was investigated by powder X-ray diffraction and HRTEM. The HRTEM images clearly show the presence of large platelets that are consistent with a layered structure often observed for metal phosphonates, such as the layered structures of $Ba(PPA)\cdot H_2O$ or $Ti(PPA)_2$. XRD data are consistent with this interpretation, and we can see the low angle 00*l* lines in the diffraction pattern shown in Figures 1 and 2 that correspond to an interlayer separation of 15.754(1) Å and 15.351(1) Å for BaTi(PPA) and SrTi(PPA), respectively. Such an interlayer spacing is consistent with a metal layer held together on both sides by phosphonic acid groups that extend into the interlayer space. A highly simplified schematic of this proposed structure is shown in Figure 10. The schematic illustrates a common mixed-metal−oxygen backbone with the phenylphosphonate groups protruding into the basal plane.

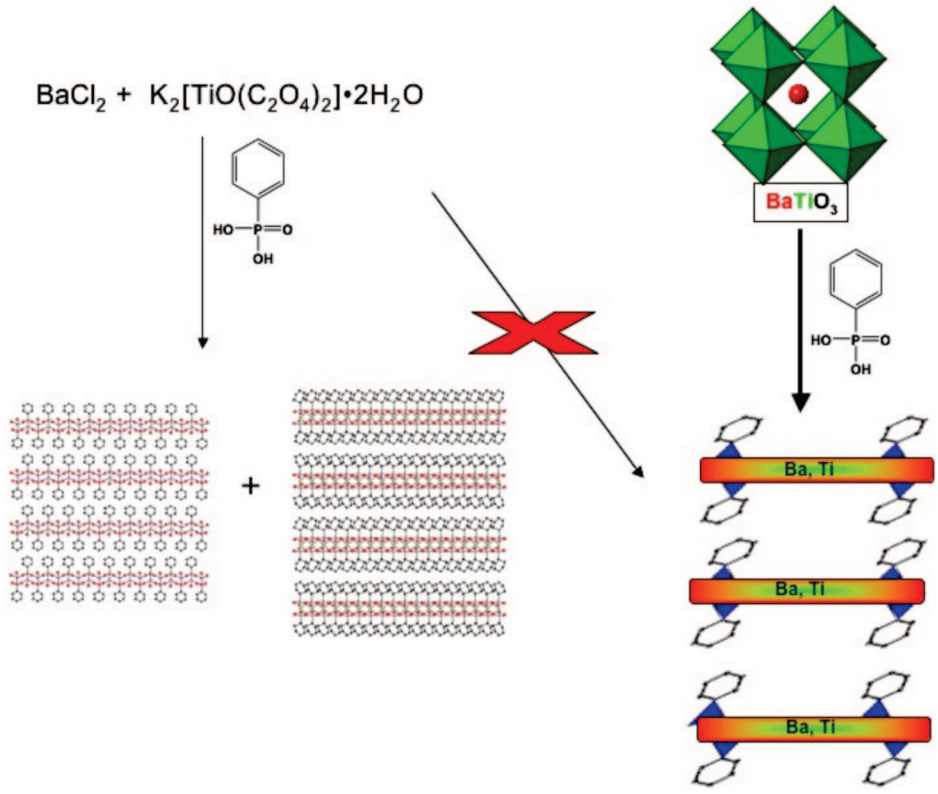

Figure 10. Schematic of the mixed-metal phosphonate structure and its synthesis.

The ^{31}P NMR data support this proposed structure consisting of barium and titanium bridged by the phenylphosphonic acid groups. The ^{31}P NMR data indicate that there are three types of phosphorus environments in these layered structures, one associated with Ba−O−P, one with Ti−O−P, and one that is thought to be due to the presence of Ba−O−P−O−Ti linkages. The "bridging-P" can be explained from reexamining the metal−oxygen−phosphorus framework in single metal phosphonates. In the divalent metal phosphonate structure, the phosphonate groups bind to the metal cations but also serve as bridging ligands to adjacent metal ions. In the case of mixed-metal centers, these bridging phosphonate groups bridge the divalent metal to the tetravalent metal.

On the basis of these data we suggest that the schematic shown in Figure 10 is a reasonable representation of the structure. Efforts to grow single crystals to determine the precise metal arrangement in the structure are under way.

The motive for synthesizing these materials is to use these layered metal phosphonates as high dielectric constant additives to generate polymer nanocomposite dielectric materials with enhanced energy density. This approach takes advantage of the high breakdown voltage of polymers and the higher dielectric constants of the metal phosphonate additives. In this study we chose polystyrene as the polymer host system to accommodate the metal phosphonate additive. Both polystyrene and $BaTi(PPA)_3$ can be dissolved/dispersed in toluene, which constitutes an effective route to thoroughly blend the platelet material into the polymer. Once dispersed in toluene and mixed with the polystyrene dissolved in toluene, it is straightforward to spin coat polymer metal phosphonate composite films, metal coat their surfaces, and measure their dielectric permittivity as a function of weight loading of the metal phosphonate.

Polystyrene films have a reported dielectric constant of ∼2−3, consistent with our measurements on spin coated polystyrene films, that gave dielectric constants of 2.55. The addition of the mixed metal phosphonates greatly increased the dielectric constant of the composite to up to ∼20 for a 40 wt % loading of $BaTi(PPA)_3$ in polystyrene, as shown in Figure 9. The corresponding strontium analogue, $SrTi(PPA)_3$ in polystyrene, reached a dielectric constant of ∼14 as seen in Figure 9. By comparison, the dielectric constants of composites made by dispersing $BaTiO_3$ or $SrTiO_3$ in polystyrene reached values of only ∼9 in both cases. Clearly, the addition of the metal phosphonate stacks to the polymer resulted in an almost 10-fold increase in the dielectric constant of the composite film.

It is important to point out that composite films prepared with single metal phosphonates, $Ti(PPA)_2$ or Ba(PPA), did not generate an improvement in the dielectric constant in excess of the $BaTiO_3$ or $SrTiO_3$ containing samples. Hence it would appear that either the presence of both metals or the structural difference between the single and the mixed metal phosphonates leads to a significant enhancement in the dielectric constant.

5. Conclusion

We have successfully synthesized a new class of mixed-metal phosphonates whose structure is closely related to those of previously reported phosphonates. Their uniqueness arises from the mixed metal content, consisting of a 1:1 ratio of divalent to tetravalent metal cations. The incorporation of

two metals into the structure enhances the dielectric constant relative to single metal phosphonates. Furthermore, polystyrene based composites containing these mixed metal phosphonates exhibit a significant enhancement in the dielectric constant as a function of increased weight loading. Work is underway to add to the family of these mixed metal phosphonates.

Supporting Information Available: Infrared spectra on the mixed-metal phenyl phosphonates; TGA and IR of the mixed metal phosphonates; HRTEM images used for the EDS analysis of the platelets; and powder X-ray diffraction patterns of the single metal phosphonates and the mixtures of the single metal phosphonates are provided in the Supporting Information section. This material is available free of charge via the Internet at http://pubs.acs.org.

Acknowledgment. Financial support for this research was provided by the Air Force award No. FA9550-08-10377 and partially through the National Science Foundation Grant IIP-0650186. Special thanks to Dr. T.S. Sudarshan, from the University of South Carolina department of Electrical Engineering, for use of the Keithley 590 CV analyzer and spin-coating device. Special thanks to Dr. Perry Pellechia, from the University of South Carolina department of Chemistry and Biochemistry, for his help with the ^{31}P MAS NMR experiments.

CM8030945